DOI 10.52209/2706-977X_2026_1_72 **IRSTI 55.03.14** **UDC 621.771**

Stress State and Contact Pressure during Asymmetrical Rolling of Thick Sheets

Ashkeyev Z.A.[1], Andreyachshenko V.A.*[2], Abishkenov M.Zh.[1], Kamarov A.U.[1]
[1] Karaganda Industrial University, Temirtau, Kazakhstan
[2]Abylkas Saginov Karaganda Technical University, Karaganda, Kazakhstan
*corresponding author

Annotation. Asymmetrical rolling is one of the modern methods of stabilizing the microstructure during the rolling process. The implementation of this process ensures an increase in the mechanical properties of rolled products, reduces texture and contributes to obtaining a more uniform microstructure. In this work, the stress state during asymmetrical rolling of thick sheets is studied and the contact pressure is determined by calculation methods. To study the stress state, the slip line method and velocity hodograph were used. Contact pressure was calculated using the slip line method. and joint solution of differential equations of equilibrium and plasticity conditions. It was revealed that in the zone of plastic deformation, compressive stress components prevail, in contrast to the traditional method of rolling in cylindrical rolls, where tensile stresses arise in the axial central zone, which can lead to destruction and elongation of grains in the rolling direction. Analysis of the calculation of contact pressures shows that the relative difference in the values of the specific contact pressures of the metal on the rolls during asymmetric rolling, calculated by the slip line method and the joint solution of differential equilibrium equations and plasticity conditions is insignificant, i.e. does not exceed 6%, which indicates the reliability of the results obtained. During asymmetrical rolling of a strip with a wide deformation zone, due to the occurrence of shear deformations, the neutral height shifts to the exit from the deformation zone, and it is even possible that there is no neutral zone.

Key words: deformation, stress state, slip lines, strain force, severe plastic deformation.

Introduction

For metallurgical production, improving product quality is of paramount importance. The production of thick plate steel is a multi-stage production process, which mainly includes steelmaking, continuous casting, hot rolling and cooling. The quality of the final product must meet the requirements for chemical components, profile, size, etc. It is determined by the technological parameters of each production stage and the quality of intermediate products. To control many factors, mechanisms such as machine learning [1], [2] and genetic algorithm [3], [4] are currently used. At the same time, the success of the production process remains directly related to the technologies used [5] - [9]. Many laboratories developing steels have focused on new high-alloy steels in which the composition and / or heat treatment dominate over the properties [10]. Another approach to improving the quality of the metal is the use of severe plastic deformation [11] - [14]. In this study, we focused on the hot rolling process. In [15], it is noted that the deformation trajectory during asymmetric rolling consists of two parts: first, the main rolling occurs, followed by a simple shear process. As is known [16] - [18], asymmetric rolling allows for the uniformity of deformation, improving the mechanical properties and microstructure of the processed workpieces [19], [20]. The first studies on the implementation of asymmetric rolling were carried out in 1948 by Sachs and Klinger [21] to develop a model of homogeneous deformation. Now the principles of asymmetric rolling are used both for steel production [22], [23] and for the processing of non-ferrous metals [24], [25], in addition, asymmetric rolling is successfully used as a basic process in accumulated rolling by joining [26], [27]. Asymmetry can be provided by the difference between the rotation speeds of the upper and lower rolls [28], different roll diameters [29], a specific roll shape leading to asymmetry [30], as well as other technological methods.

Despite the increased attention to the asymmetric rolling process, the stress-strain state during asymmetric rolling, as well as the values of contact pressure, which are necessary for the correct design of the rolling process, remain insufficiently studied. Thus, in [31], the configuration zones of deformation in the process of asymmetric rolling were analyzed, the authors [32] performed a modeling of friction forces in two-roll modules, where asymmetry is provided by the arrangement of rolls of different diameters. Despite the use of asymmetric rolling as a heterogeneity regulator, asymmetric rolling itself is also accompanied by a heterogeneous stress-strain state [33], and the magnitude of asymmetry can affect the magnitude of the shift [34].

The aim of the work: to study the stress state during asymmetric rolling of thick sheets and to determine the contact pressure using calculation methods.

1. Experimental part

The process of asymmetric strip rolling has a positive effect on the quality of the metal, i.e. on the mechanical and geometric properties of the resulting rolled metal products and the power parameters of the process. Let us consider the stress state and change in contact pressure of thick strips during asymmetric rolling.

The production of thick strips and blanks occupies a significant place in the national economy, as they are widely used in the oil and gas industry, shipbuilding, bridge building, mechanical engineering and other industries. Therefore, the quality of the resulting rolled metal products is increasingly demanding. One of the ways to solve this problem is the process of asymmetric rolling of blanks in conical rolls with different variable diameters along the length of the roll barrel. Asymmetric rolling can also be used in the processing of composite materials to ensure the required quality.

To study the stress state, the slip line (SL) method and the velocity hodograph were used. The contact pressure was calculated using the SL method and the joint solution of the differential equations of equilibrium and the plasticity condition. When determining the stress state using the slip line method, the following properties are used:

1 Slip lines form two mutually perpendicular families of curves α and β;

2 Slip lines must be continuous;

3 Slip lines must be orthogonal;

4 Slip lines must intersect the direction of the principal normal stresses at an angle of π/4;

5 The change in the average normal stress σcp when moving along the slip line is equal to the product of its angle of rotation by 2k.

Let us consider one of the options for asymmetric rolling of thick strips, adopting the following main parameters that characterize the proposed process:

1. The diameter of the larger roll D = 980 mm, the strip reduction $\Delta h = h_0 - h_1 = 10$ mm, where h_0 is the initial strip thickness, h_1 is the final strip thickness, the degree of reduction $\varepsilon_h = \Delta h/h_0 = 10/40 = 0.25$ and the length of the contact arc $l_D = \sqrt{R\Delta h} = \sqrt{490 \cdot 10} = 70$ mm, where R is the radius of the larger roll.

2. The diameter of the smaller roll d = 720 mm, the length of the contact arc $l_d = \sqrt{r\Delta h} = \sqrt{360 \cdot 10}$=60 mm, the length of the roll barrel L_b = 1500 mm, the taper of the rolls, $\frac{(D-d)}{2L_b}$= 0.04924, i.e. γ = arctg(0.04924) = 4.95 ≈ 5°, which is the most optimal value, since with increasing taper, the feeding and gripping of the strip by the rolls becomes more difficult.

3. The angle of gripping the strip, respectively, from the side of the larger diameter and the length of the contact arc: $\alpha_D = arccos[1-(\frac{\Delta h}{2R})]$=8°192, $l_D = \frac{\pi R\alpha_D}{180} = \frac{\pi \cdot 490 \cdot 8{,}192}{180}$ =70,02 mm.

4. The angle of capture from the side of the smaller diameter and the length of the contact arc, $\alpha_d = arccos[1-(\frac{\Delta h}{2r})]$=9°56, $l_d = \frac{\pi r\alpha_r}{180} = \frac{\pi \cdot 360 \cdot 9.56}{180}$ =60.04 mm.

The obtained values of the length of the contact arc from the side of the larger and smaller diameters, calculated by two expressions are identical and practically coincide, accordingly they can be considered correct.

A distinctive feature of the proposed process of asymmetric rolling of thick strips from the known ones [30] is that the shape of the deformation zone is wide, i.e., the ratio of the average contact arc length to the mean strip thickness is $\frac{(l_D+l_d)}{(h_0+h_1)}$= 1.85, in contrast to conventional processes, where the deformation zone is narrow and does not exceed $\frac{(l_D+l_d)}{(h_0+h_1)}$ ≈1,0.

Therefore, it is of interest to determine the stress state and contact pressure during asymmetric rolling of thick sheets with a wide shape of the plastic deformation zone *abcd* (Fig. 1), since the use of thick sheets in production is increasing (armor, shipbuilding, etc.). The field of slip lines (SL) during rolling of thick strips is shown in Fig. 1.

The construction of the slip-line field is carried out from the strip exit side of the plastic deformation zone, where the slip lines intersect the principal *x*- and *y*-axes at the nodal point 0.0′ at an angle of 45° (Fig. 1).

The construction of the SL grid is performed from the side of the strip exit from the plastic deformation zone, where the SL must intersect with the principal axes x and y at the nodal point 0.0' at an angle of 45°. Taking the step of change of LS equal to Δθ'=2Δθ=20°, or π/9 rad, and drawing from points *b* and *d* arcs with radii: /*b* 0.0′/ and /*d* 0.0′/ at an angle of 2Δθ=20°, we obtain nodal points 0.1' and 1.1'. By replacing the obtained arcs with chords, perpendiculars are drawn from the resulting points (0.1′ and 1.1′) to the chords until they intersect the x-axis; as a result, the intersection point 2.4 is obtained (Fig. 1).

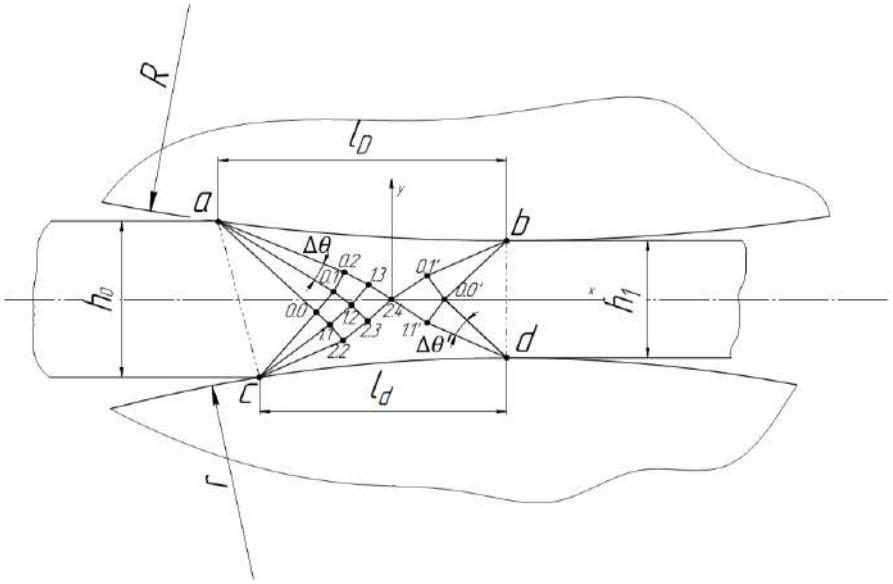

R – radius of the larger roll; r – radius of the smaller roll; l_d, l_D – the length of the contact arc ; h_0, h_1 – initial and final strip thickness

Fig. 1 – Field of slip lines during asymmetric rolling of thick strips

When constructing, we strictly used the basic properties of the LS, for example, the orthogonality property, i.e. the property of the LS intersection with the main axes at a right angle, etc. Using the LS properties, we construct the SL grid by analogy from the side of the entrance to the plastic deformation zone, up to the intersection with the nodal point 2.4. From the constructed SL grid, it can be seen that the number of nodal points from the side of the entrance to the plastic deformation zone is greater than from the exit side. This can be explained by the fact that closer to the exit, the plastic deformation process is completed and the strip moves as an absolutely rigid body. The correctness of the SL grid can be verified by constructing the velocity field. Figure 2 shows the velocity hodograph. The velocity plan was also constructed using the basic properties of the SL, i.e. the orthogonality property. On the y-axis, vertically, we plot the roll speed $\dot{u}_0$, equal to the value of strip compression per unit time t, i.e. $\dot{u}_0 0=\Delta h/t$. We construct from the side of the strip exit from the plastic deformation zone to the nodal point 0.0', observing the orthogonality condition. Hence, if we neglect the change in width during rolling, we can write the incompressibility condition for a unit of strip width.

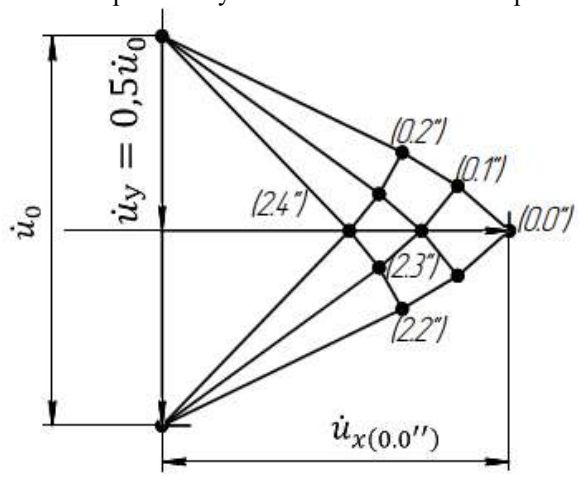

Fig.2 – Speed hodograph for rolling in conical rolls

The incompressibility condition can be written as follows:

$$\dot{u}_0 \cdot l_{mean} = \dot{u}_{x(0.0'')} \cdot h_{mean}, \text{ hence, } \frac{l_{mean}}{h_{mean}} = \frac{\dot{u}_{x(0.0'')}}{\dot{u}_0} = \frac{(l_D+l_d)}{(h_0+h_1)} = \frac{\dot{u}_{x(0.0'')}}{\dot{u}_0} \approx 1.850.$$

It can be seen that taking into account the error, the incompressibility condition is satisfied, which indicates the correctness of the constructed LS grid. Next, we can proceed to calculating the stresses in the plastic deformation zone *abcd*. From the condition of equilibrium of forces at the exit from the plastic deformation zone, we can write the following,

$$\int_{0.0'}^{b} \sigma_{0.0'}\, dy + kx_b = 0,$$

$$\sigma_{0.0'}\,(y_{0.0'} - y_b) + kx_b = 0,$$

$$\sigma_{0.0'}\,(-y_b) = kx_b, \text{ as } y_{0.0'} = 0, \text{ thence,}$$

$$\sigma_{0.0'} = -k = -\frac{\sigma_T^*}{2},$$

since $x_b = y_b$, where σ_t^* is the deformation resistance depending on the temperature-speed and deformation parameters of the rolling process. Assuming that a strip of Steel 45 is rolled at a temperature of 1000 °C, with a thickness reduction of ε_h = 25% and a strain rate of $\dot{u}$=1s^{-1}, the deformation resistance is σ_T^*= 85 MPa.

Knowing the average stress at the nodal point 0.0', from the Hencky relation one can determine the average stress at the neighboring nodal point 1.1', i.e.,

$$\sigma_{1.1'} = \sigma_{0.0'} - 2k\Delta\theta',$$

$$\sigma_{1.1'} = -k - 2k\frac{\pi}{9} = -\frac{\sigma_t^*}{2}\left(1 + 2\frac{\pi}{9}\right) = -1{,}7\frac{\sigma_t^*}{2}.$$

The average stress at the nodal point 1.1' increases by 1.7 times compared to the value at the nodal point 0.0', which once again proves the advantage of asymmetric rolling.

From the condition of equilibrium of forces from the larger and smaller roll diameters, the average stresses at the nodal points 1.1' and 0.1' will be equal. From the condition of symmetry and equilibrium of forces relative to these axes, similar values of the average stresses will also be at the nodal points 0.2. and 1.2. Given the metal deformation resistance σ_T^*= 85 MPa, the mean stress at the nodal points $0.0'$and 0.0, is determined as k=- $\frac{\sigma_T^*}{2}$ = -42,5 MPa. From the symmetry of the points and the orthogonality of the LS at the nodal points 0.2, 2.2, 0.1' and 1.1' will be equal to:

$$\sigma_{1.1'} = \sigma_{0.1'} = \sigma_{0.2} = \sigma_{2.2} = 1.7\frac{85}{2} = -72.25, \text{ MPa.}$$

It will be slightly lower at the intermediate nodal points 0.1 and 1.1, determined through the rotation angle of the hp $\Delta\theta$=10° (π/9 rad), as follows:

$$\sigma_{1.1} = \sigma_{0.1} = -k - k\frac{\pi}{9} = -\frac{\sigma_t^*}{2}\left(1 + \frac{\pi}{9}\right) = -57.327 \text{ MPa.}$$

The voltage components at the corresponding nodal points are determined using the following expressions:
At the nodal point 0.0',

$$\sigma_{x0.0'} = \sigma_{0.0'} + k\sin 2\theta_{0.0'} = -k + k = 0;$$
$$\sigma_{y0.0'} = \sigma_{0.0'} - k\sin 2\theta_{0.0'} = -k - k = -2k = -85 \text{ MPa};$$
$$\tau_{xy0.0'} = -k\cos 2\theta_{0.0'} = 0,$$

where θ_(0.0') is the angle of inclination of the hp to the principal axes at the nodal point 0.0', which at this point is equal to 45°.

At the adjacent nodal point 0.1',

$$\sigma_{x0.1'} = \sigma_{0.1'} + k\sin 2\theta_{0.1'} = -72.25 + 72.25\sin 2\cdot(45+20) = -16.904 \text{ MPa};$$
$$\sigma_{y0.1'} = \sigma_{0.1'} - k\sin 2\theta_{0.1'} = -72.25 - 72.25\sin(2\cdot 65) = -127.596 \text{ MPa};$$
$$\tau_{xy0.0'} = -k\cos 2\theta_{0.1'} = 27.318 \text{ MPa.}$$

At the intermediate nodal point 0.1 and 1.1,

$$\sigma_{x0.1} = \sigma_{0.1} + k\sin 2\theta_{0.1} = -57.327 + 57.327\sin 2\cdot(45+10) = -3.457 \text{ MPa};$$
$$\sigma_{y0.1} = \sigma_{0.1} - k\sin 2\theta_{0.1} = -57.327 - 57.327\sin(2\cdot 55) = -111.197 \text{ MPa};$$

$$\tau_{xy0.0'} = -k\cos 2\theta_{0.1} = 14.535 \text{ MPa}.$$

Analysis of the distribution of stress components shows that all values of stress components increase from the center to the contact surface. By summing the stress components along the y axis, we can calculate the average contact stress p_{mean} and the rolling force, i.e.,

$$p_{mean} = \frac{(85+111,197+127,596)}{3} = 107.931 \text{ MPa}.$$

It should be noted that in the plastic deformation zone *abcd* the stress components are compressive, unlike the traditional rolling method in cylindrical rolls, where tensile stresses arise in the axial central zone, which can lead to destruction and stretching of grains in the rolling direction.

When rolling a wide strip, the compressive stresses acting in the plastic deformation zone are more significant, compared to a narrow shape of the plastic deformation zone. This is due to the fact that with a low shape of the deformation zone, the coverage is denser, which does not allow the development of tensile stresses. Especially in the axial central zone of the strip, where during symmetrical rolling in cylindrical rolls, significant tensile stresses arise, which lead to the destruction of the metal in the rolling direction.

Therefore, to prevent this phenomenon, it is advisable to roll in conical rolls with different diameters along the length of the roll barrel.

To determine the specific contact pressure of the metal on the rolls, we use the method of jointly solving the differential equations of equilibrium and the plasticity condition. To do this, let us consider the equilibrium condition of the element a'b'c'd', located at a distance x from the center p of the *x* and *y* coordinate axes (Fig. 3).

The following forces act on the selected element a'b'c'd':

From the side of the entrance to the plastic deformation zone, $(\sigma_x+d\sigma_x)\frac{h_x}{cos\beta}$;

From the side of the exit from the plastic deformation zone, $\sigma_x(h_x-dh_x)$;

The component of the contact pressure p along the x axis from the side of the larger diameter of the rolls, $p\sin\varphi_x\frac{dx}{cos\varphi_x}$;;

The component of the contact pressure p along the x axis from the side of the smaller diameter of the rolls, $p\sin\varphi_{x1}\frac{dx_1}{cos\varphi_{x1}}$;

The contact friction forces from the side of the larger diameter rolls, $t_x\cos\varphi_x\frac{dx}{cos\varphi_x}$;

Contact friction forces from the side of the smaller diameter rolls, $t_x\cos\varphi_{x1}\frac{dx_1}{cos\varphi_{x1}}$.

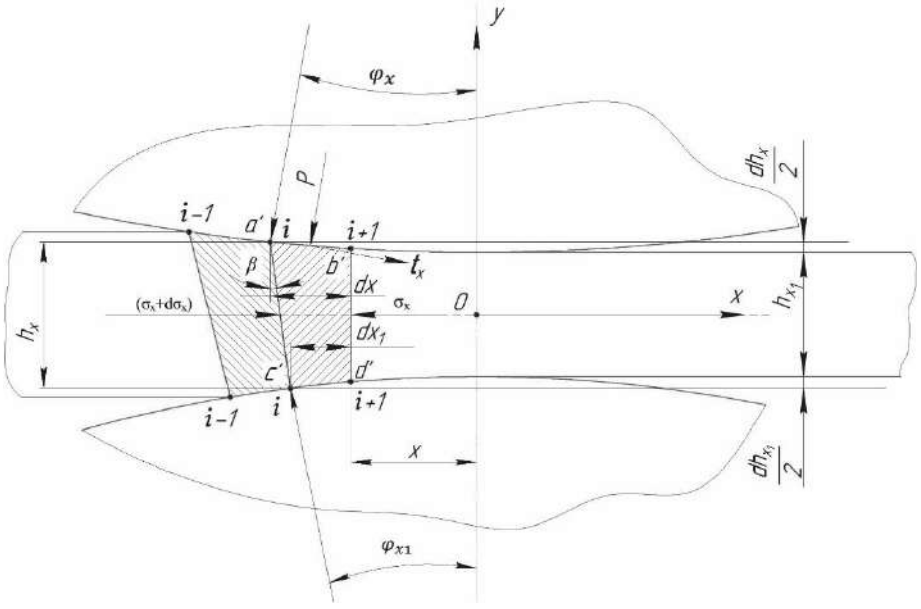

Fig.3 – The equilibrium condition of the element a'b'c'd' and the step of changing the nodes of the grids *i-1*, *i*, *i+1* in the center of plastic deformation during asymmetric rolling of thick sheets

From the condition of equilibrium of the element, a'b'c'd' we can write the following:

$(\sigma_x+d\sigma_x)\frac{h_x}{cos\beta}-\sigma_x(h_x-dh_x)+t_x cos\varphi_x\frac{dx}{cos\varphi_x}+t_x cos\varphi_{x1}\frac{dx_1}{cos\varphi_{x1}}-psin\,\varphi_x\frac{dx}{cos\varphi_x}-psin\,\varphi_{x1}\frac{dx_1}{cos\varphi_{x1}}=0$, or,

$(\sigma_x+d\sigma_x)\frac{h_x}{cos\beta}-\sigma_x(h_x-dh_x)+t_x(dx+dx_1)-ptg\,\varphi_x dx-ptg\,\varphi_{x1}dx_1)=0.$

Using the following relationships, i.e. $tg\varphi_x=\frac{dh_x}{2dx}$ and $tg\varphi_{x1}=\frac{dh_{x_1}}{2dx_1}$, as well as the Coulomb-Amontons law in the following form, $t_x=\mu p$, then the differential equation can be represented as follows:

$\sigma_x\frac{h_x}{cos\beta}+d\sigma_x\frac{h_x}{cos\beta}-\sigma_x h_x+\sigma_x dh_x+\mu p\frac{dh_x}{2}\left(\frac{1}{tg\varphi_x}+\frac{1}{tg\varphi_{x1}}\right)-pdh_x=0,$

where $dh_x=\frac{dh_x}{2}+\frac{dh_{x_1}}{2}-$ elementary strip compression.

In the case under consideration, the angle β≈14°, then cosβ=0.97≈1.0, the differential equation is simplified to the following form:

$d\sigma_x h_x+\sigma_x dh_x+\mu p\frac{dh_x}{2}\left(\frac{1}{tg\varphi_x}+\frac{1}{tg\varphi_{x1}}\right)-pdh_x=0$, after reducing by h_x, we get:

$d\sigma_x+\sigma_x\frac{dh_x}{h_x}-p\left(1-\frac{\mu}{2tg\varphi_x}-\frac{\mu}{2tg\varphi_{x1}}\right)\frac{dh_x}{h_x}=0.$

Using the plasticity condition $p-\sigma_x=\sigma_т^*$ or $\sigma_x=p-\sigma_т^*$, by $\sigma_т^*$=const $dp=d\sigma_x$, we will receive,

$dp+[(p-\sigma_т^*)-p\left(1-\frac{\mu}{2tg\varphi_x}-\frac{\mu}{2tg\varphi_{x1}}\right)]\frac{dh_x}{h_x}=0.$

$dp+[p\left(\frac{\mu}{2tg\varphi_x}+\frac{\mu}{2tg\varphi_{x1}}\right)-\sigma_т^*]\frac{dh_x}{h_x}=0.$

To solve the obtained differential equation, we will use the numerical method of finite differences or the grid method, where for the grid points we compose a finite difference analogue in the following form:

$$\Delta p_i=[\sigma_т^*-p_i\left(\frac{\mu}{2tg\varphi_x}+\frac{\mu}{2tg\varphi_{x1}}\right)]\frac{\Delta h_{xi}}{h_{xi}}. \quad (1)$$

Then, at the corresponding grid nodal points, this expression can be expanded as follows:

$$(p_{i-1}-p_i)=[\sigma_т^*-p_i\left(\frac{\mu}{2tg\varphi_{xi}}+\frac{\mu}{2tg\varphi_{x1i}}\right)]\frac{h_{xi-1}-h_{xi}}{h_{xi}}, \quad (2)$$

for example, when i=1,

$$(p_0-p_1)=[\sigma_т^*-p_1\left(\frac{\mu}{2tg\varphi_{x1}}+\frac{\mu}{2tg\varphi_{x11}}\right)]\frac{h_0-h_1}{h_1}, \quad (3)$$

for example, when i=2,

$$(p_1-p_2)=[\sigma_т^*-p_2\left(\frac{\mu}{2tg\varphi_{x2}}+\frac{\mu}{2tg\varphi_{x12}}\right)]\frac{h_1-h_2}{h_2}, \quad (4)$$

etc. from the initial height of the strip $h_{i-1}=h_0$=40 mm, from the side of the entrance to the deformation zone (lag zone) and to the neutral height of the strip $h_{i-1}=h_n$, where the contact pressures from the lag and lead zones must be equal.

For step-by-step calculation of the contact pressure p_i, the section of the deformation zone length is divided into n steps, respectively from the side of the larger and smaller diameters of the rolls, i.e.: $\Delta x_i=\frac{l_D}{n}$ and $\Delta x_{i1}=\frac{l_d}{n}$, where n – number of steps. For this case under consideration, we first take n=10, then, $\Delta x_i=\frac{70}{10}=7$ mm and $\Delta x_{i1}=\frac{60}{10}$=6 mm. Accordingly, the step of changing the elementary compression of the strip will be equal to, $\Delta h_{xi}=\frac{10}{10}$= 1,0 mm. Then, the step of changing the angles, respectively, from the side of the larger and smaller diameters, respectively, will be equal to: $tg\varphi_{x1}=\frac{1}{2*7}$=0,0714, $tg\varphi_{x11}=\frac{1}{2*6}$=0.0833, the step of change of which is unchanged, and remains constant during further step-by-step calculation.

At both ends of the plastic deformation zone, the values of normal pressure pi and pi+1 are known and equal, i.e., $p_0=p_{10}=\sigma_t^*$= 85 MPa. Taking into account the accepted values and designating the values in brackets in equations (1-4) with the letter $\delta=\left(\frac{\mu}{2tg\varphi_x}+\frac{\mu}{2tg\varphi_{x1}}\right)$ =3.25, (μ – coefficient of contact friction) equation (1) can be represented as follows:

$$\frac{\Delta p_i}{(\sigma_t^*-p_i\delta)}=\frac{\Delta h_{xi}}{h_{xi}}. \quad (5)$$

Thus, knowing the initial values and the step of changing the elementary length of the deformation zone, the angles of capture and the height of the strip, it is possible to calculate the corresponding values of p_i at the corresponding nodal points plotted on the grid of the plastic deformation zone (Fig. 3) step by step.

Let us make the first step to determine the contact pressure p1: at n = 10, i = 1, Δh_x = 1 = 1.0 mm, h_{xi} = 1 = 39 mm, at the average value of the contact friction coefficient μ = 0.25. We will start the calculation from the side of the entrance to the deformation zone, i.e. from the lagging zone to the neutral height of the strip

$h_n = h_{xi=5}$=35 mm:

$(85 - p_1) = [\,85 - p_1(3.25)]\frac{1}{39}$, from here p_1 =90.35 MPa.

We perform the calculation in the next step at i=2,

$(90.35 - p_2) = [\,85 - p_2(3.25)]\frac{1}{38}$, from here p_2=96.35 MPa.

We perform similar calculations when i=3,

$(96.35 - p_3) = [\,85 - p_3(3.25)]\frac{1}{37}$, from here p_3 =103.11 MPa, etc. up to the neutral height of the strip, where the contact pressures should be equal. Further assuming that it is in the middle of the plastic deformation zone, i.e. $h_n = h_{xi=5} \approx 35$ mm, we get it p_5 =119.40≈120 MPa.

A similar differential equation of equilibrium, changing the sign, can be written from the side of the exit from the plastic deformation zone, i.e. from the side of the advance zone. For this, we use the obtained finite-difference analogue (2), representing it as follows:

$$(p_{i+1} - p_i) = [\,\sigma_t^* - p_i(3.25)]\frac{h_{xi} - h_{xi+1}}{hx_i}$$

We will also similarly perform the first step of calculating the contact pressure pi, from the exit side of the plastic deformation zone. *abcd* i.e. when i=9,

$$(85 - p_9) = [\,85 - p_9(3.25)]\frac{1}{31}, \text{ from here } p_9 = 91.9 \text{ MPa.}$$

It can be seen that at the first step from the lagging zone the contact pressure was p_1 =90.35 MPa, and the difference is less than 2%.

Let's perform the next step of calculation at the nodal point i=8,

$(91.9 - p_8) = [\,85 - p_8(3.25)]\frac{1}{32}$, и p_8= 99.32 MPa.

Let's take the next counter step i=7,

$(99.32 - p_7) = [\,85 - p_7(3.25)]\frac{1}{33}$, and p_7= 107.315 MPa.

2.Discussing the results

The contact pressure values at the adopted neutral height of the strip from the lead zone side at $h_n = h_{xi}$=5=35 mm are equal to p_5 = 125.07≈125 MPa.

Based on the fact that the neutral line of the strip is presumably located between h_{x-1} and h_{x+1}, i.e. between the current height of the strip: 36÷34 mm, it should be expected that the maximum value of the contact pressure will also be between the obtained values, i.e. between 120 and 125 MPa, where the difference between the obtained values is 4%. To accurately determine the neutral height h_n, it is necessary to reduce the step of changing the adopted values. With a further decrease in the adopted values, to Δx_i=70/20=3.5 mm, Δx_{i1}=60/20 =3 mm, Δh_{xi}=10/20 = 0.5 mm, i.e. taking the number of steps n=20, at $h_n = h_{xi}$=10≈34.5 mm, the contact pressure from the lagging zone side will be 122.65 MPa, and from the leading side: ~120.0 MPa, i.e. the difference will already be about 2%.

Similarly, as in the previous case, summing up the value of the contact pressure along the contact surface, we obtain the average value, which will be equal to p^*_{mean}≈ 101.94 MPa. Approximately the same value was obtained above by the hp method (p_{mean}=107.93 MPa), i.e. the difference does not exceed 6%.

The slip-line method, on the other hand, offers a clear analytical framework and allows for a transparent visualization of the stress and strain fields. Therefore, while both methods yield close results, the combined differential-equation approach can be considered slightly more accurate for detailed local stress predictions, whereas the slip-line method is valuable for understanding the overall physical behavior and for parametric studies.

Analysis of the calculation of contact pressures shows that the relative difference in the values of specific contact pressures of metal on the rolls during asymmetric rolling, calculated by the hp method and the joint solution of the

differential equations of equilibrium and the plasticity condition, is insignificant, i.e. does not exceed 6%, which indicates the reliability of the results obtained.

It should be noted that, in asymmetric strip rolling with a wide deformation zone, the neutral plane shifts (rotates) toward the exit of the plastic deformation region due to the development of shear strains. Determining the position of this surface therefore constitutes the next principal task, which must be considered separately. Relative to the neutral height of the strip during symmetrical rolling, tensile stresses arise in the direction of rolling, which can lead to ruptures and cracks in the direction of rolling. Therefore, to transform these undesirable phenomena, it is effective to use asymmetrical rolling to ensure the required quality of rolled metal.

Conclusions

In asymmetric rolling of strips with a wide deformation zone, the compressive stresses are significantly higher compared to a narrow deformation zone. This is due to the denser contact between the rolls and the strip in the wide deformation zone, which prevents the development of tensile stresses. This effect is particularly important in the central axial zone of the strip, where symmetric rolling in cylindrical rolls can generate considerable tensile stresses that may lead to cracks and material failure.

The contact pressures calculated using the slip-line method and the combined solution of the differential equilibrium equations with the plasticity condition differ by no more than 6%. This confirms the correctness of the obtained results and allows accurate determination of rolling forces and torques, which is critical for evaluating the strength and durability of the main components of the rolling mill during the production of thick strips.

It should be noted that the numerical solution of the differential equations provides higher local accuracy, while the slip-line method offers a clear and convenient visualization of the stress distribution across the strip. The shift of the neutral line toward the exit of the plastic deformation zone due to shear deformations is an important factor affecting the stress distribution and requires separate investigation.

Future research may focus on refining the neutral line position, accounting for strain hardening, variable friction, and temperature gradients to improve predictive accuracy and optimize the asymmetric rolling process.

Acknowledgement

The work was carried out within the framework of the state budget research work AP19677907 “Study of the influence of micro/nanoparticles, industrial waste and shear on the quality of metal blanks for mechanical engineering”.

References

[1] Ji Yi., Liu Sh., Zhou M., Zhao Z., Guo X., Qi L. A machine learning and genetic algorithm-based method for predicting width deviation of hot-rolled strip in steel production systems //Information Sciences, 2022, 589. - p. 360-375. https://doi.org/10.1016/j.ins.2021.12.063.

[2] Pan Q.-K., Gao L., Wang L. A multi-objective hot-rolling scheduling problem in the compact strip production //Applied Mathematical Modelling, 2019, 73. – p. 327-348. https://doi.org/10.1016/j.apm.2019.04.006.

[3] Liu X., Xiao H. Theoretical and experimental study on the producible rolling thickness in ultra-thin strip rolling //Journal of Materials Processing Technology, 2020, 278 – p. 116537. https://doi.org/10.1016/j.jmatprotec.2019.116537.

[4] Muntin A.V. Advanced Technology of Combined Thin Slab Continuous Casting and Steel Strip Hot Rolling //Metallurgist, 2019, 62. – p. 900–910. https://doi.org/10.1007/s11015-019-00747-5.

[5] Mekhtiev A.D., Yurchenko A.V., Neshina E.G., Al’kina A.D., Madi P.Sh. Physical Principles of Developing Pressure Sensors Using Refractive Index Changes in Optical Fiber Microbending //Russian Physics Journal, 2020, 63.2. – p. 323–331 https://doi.org/10.1007/s11182-020-02038-y.

[6] Mekhtiev A., Alkina A., Neftissov A., Kazambayev I., Kirichenko L. Intelligent Systems for Monitoring the Integrity of Technical Objects Based on Distributed Fiber-Optic Sensors. CEUR Workshop Proceedings, 2022, 3347. – p. 290-306.

[7] Yurchenko A.V., Mekhtiyev A.D., Bulatbaev F.N., Neshina Y.G., Alkina A.D. Investigation of Additional Losses in Optical Fibers Under Mechanical Action //IOP Conference Series: Materials Science and Engineering, 2019, 516.1 – p. 012004. https://doi.org/10.1088/1757-899X/516/1/012004.

[8] Yurchenko A., Alkina A., Mekhtiev A., Bulatbayev F., Neshina E. The Questions of Development of Fiberoptic Sensors for Measuring Pressure with Improved Metrological and Operational Characteristics //MATEC Web of Conferences, 2016, 79. – p. 01085. DOI: 10.1051/matecconf/20167901085.

[9] Mekhtiev A., Bulatbaev F.N., et all. Use of reinforcing elements to improve fatigue strength of steel structures of mine hoisting machines (MHM) //Metallurgija, 2020, 59.1 – p.121-124.

[10] Zhu Y., et al. Rapid alloy prototyping for strip steel development: DP800 steel case study //Ironmaking & Steelmaking, 2021, 48.5 – p. 493-504.

[11] Andreyachshenko V., Naizabekov A.B. Microstructural and mechanical characteristics of AlSiMnFe alloy processed by equal channel angular pressing. Metalurgija, 2016, 55(3). – p. 353–356.

[12] Andreyachshenko V.A. Evolution of the AA2030 alloy microstructure in the ECAP process //.Kovove Materialy, 2022, 60(2). – p. 79-87. doi: 10.31577/km.2022.2.79.

[13] Andreyachshenko V.A. Finite element simulation (FES) of the fullering in device with movable elements //Metalurgija, 2016.55(4) – 829–831.
[14] Sachs G., Klingler, L.J. The Flow of Metals Through Tools of Circular Contour //ASME. J. Appl. Mech., 1947, 14(2) – pp. A88–A98. https://doi.org/10.1115/1.4009656.
[15] Ren X., Zhang X., Huang Yu., Liu Yu, Zhao L., Zhou W. Evolution of shear texture during the asymmetric rolling and its annealing behavior in a twin-roll casting AA6016 sheet: an ex-situ electron backscatter diffraction study //Journal of Materials Research and Technology, 2020, 9, 3. – p. 6420-6433. https://doi.org/10.1016/j.jmrt.2020.04.026.
[16] Fu B., Pei C., Pan H., Guo Y., Fu L., Shan A. Hall-Petch relationship of interstitial-free steel with a wide grain size range processed by asymmetric rolling and subsequent annealing. Materials Research Express, 2020, 7(11). – p. 116516. DOI 10.1088/2053-1591/abc79f.
[17] Dhinwal S.S, Toth L.S., Lapovok R., Hodgson P.D. Tailoring One-Pass Asymmetric Rolling of Extra Low Carbon Steel for Shear Texture and Recrystallization //Materials, 2019, 12(12) – p. 1935. https://doi.org/10.3390/ma12121935.
[18] Ashkeyev Z.A., Andreyachshenko V.A., Bukanov Z.U. Research of the asymmetric rolling of workpieces // PNRPU Mechanics Bulletin, 2020, 4. – p. 27–35.
[19] Vincze G., Simões F.J.P., Butuc M.C. Asymmetrical Rolling of Aluminum Alloys and Steels: A Review. Metals, 2020, 10(9). – p.1126. https://doi.org/10.3390/met10091126.
[20]Zhu J., Liu Sh., Long D., Zhou Sh., Zhu Yu., Orlov D. The evolution of texture and microstructure uniformity in tantalum sheets during asymmetric cross rolling // Materials Characterization, 2020, 168. – p. 110586. https://doi.org/10.1016/j.matchar.2020.110586.
[21] Magalhães D.C.C., Sordi V.L., Kliauga A.M. Microstructure evolution of multilayered composite sheets of AA1050/AA7050 Al alloys produced by Asymmetric Accumulative Roll-Bonding //Materials Characterization, 2020, 162. – p. 110226. https://doi.org/10.1016/j.matchar.2020.110226.
[22] Magalhães D.C.C., Cintho O.M., Rubert J.B., Sordi V.L., Kliauga A.M. The role of shear strain during Accumulative Roll-Bonding of multilayered composite sheets: Pattern formation, microstructure and texture evolution //Materials Science and Engineering: A, 2020, 796 – p. 140055. https://doi.org/10.1016/j.msea.2020.140055.
[23] Vincze G., Pereira A.B., Lopes D.A.F,. Yánez J.M.V., Butuc M.C. Study on Asymmetric Rolling Process Applied to Aluminum Alloy Sheets. Machines, 2022, 10(8). – p.641. https://doi.org/10.3390/machines10080641.
[24] Choi C.H., Kim K.H., Lee D.N. The effect of shear texture development on the formability in rolled aluminum alloy sheets. //Mater. Sci. Forum, 1998, 273–275. – p. 391–396. https://doi.org/10.4028/www.scientific.net/MSF.273-275.391.
[25] Pustovoytov D., Pesin A., Tandon P. Asymmetric (Hot, Warm, Cold, Cryo) Rolling of Light Alloys: A Review. Metals, 2021, 11(6) – p. 956. https://doi.org/10.3390/met11060956.
26. Wang J., Liu X., Sun X. Study on the relationship between asymmetrical rolling deformation zone configuration and rolling parameters // International Journal of Mechanical Sciences, 2020, 187. – p. 105905. https://doi.org/10.1016/j.ijmecsci.2020.105905.
[27] Khurramov Sh.R., Abdukarimov A., Khalturaev F.S., Kurbanova F.Z. Modeling of friction forces in an asymmetric two-roll module //IOP Conference Series: Materials Science and Engineering, 2020, 916, No. 1 – p. 012051. DOI 10.1088/1757-899X/916/1/012051.
[28] Mavlonov T., Akhmedov A., Saidakhmedov R., Bakhadirov K. Simulation modelling of cold rolled metal strip by asymmetric technology In IOP Conference Series: Materials Science and Engineering //International Scientific Conference Construction Mechanics, Hydraulics and Water Resources Engineering (CONMECHYDRO – 2020), 23-25 April 2020, Tashkent, Uzbekistan, 883 – p. 012194. DOI 10.1088/1757-899X/883/1/012194.
[29] Wang X., Liu H., Tang X., Wang Y., Guo M., Zhuang L. Influence of asymmetric rolling on the microstructure, texture evolution and mechanical properties of Al–Mg–Si alloy //Materials Science and Engineering: A, 2022, 844 – p. 143154. https://doi.org/10.1016/j.msea.2022.143154.
[30] Khurramov Sh.R. Some questions of the contact interaction theory in two-roll modules //J. Phys.: Conf. Ser., 2020, 1546. – p. 012132. DOI 10.1088/1742-6596/1546/1/012132.

Information of the authors

Ashkeyev Zhassulan Amanzholovich, c.t.s., ass. professor, docent, Karaganda Industrial University
e-mail: jashkeev@mail.ru

Andreyachshenko Violetta Alexandrovna, PhD, associate professor, head of the test laboratory of engineering profile «Complex development of mineral resources», Abylkas Saginov Karaganda technical university
e-mail: v.andreyachshenko@ktu.edu.kz

Abishkenov Maxat Zharylgasynovich, PhD, senior lecturer of the department of "Technological machines and transport", Karaganda Industrial University
e-mail: m.abishkenov@tttu.edu.kz

Kamarov Aman Uakhitovich, doctoral student of the department of "Technological machines and transport", Karaganda Industrial University
e-mail: a.kamarov@tttu.edu.kz